

ANALYSIS OF *HUBBLE* SPACE TELESCOPE FINE GUIDANCE SENSOR DATA IN TRANS MODE: AN OVERVIEW

Elliott P. Horch¹

RESUMEN

El Sensor para el Guiado Fino del Telescopio Espacial Hubble ha sido un instrumento muy productivo en el campo de las estrellas binarias. En este trabajo el autor describe el instrumento brevemente y discute el formato de datos de las observaciones en modo TRANS. Este modo es empleado para la realización de observaciones conducentes a la obtención de la astrometría relativa de estrellas binarias con baja separación angular. Los procedimientos de análisis de datos típicamente usados son discutidos aquí y se introduce además una nueva técnica para la determinación de los colores de las componentes de estrellas binarias, basada en el análisis de Fourier.

ABSTRACT

The Fine Guidance Sensor (FGS) system on the *Hubble* Space Telescope (*HST*) has been an extremely productive instrument for binary star astronomy. This paper will briefly describe the instrument and discuss the data format for TRANS mode observations, which is used for relative astrometry observations of close binary stars. The data analysis procedures that are typically used will be covered, and a new Fourier-based technique that may be capable of determining component colors of binaries in certain situations will be introduced.

Key Words: **BINARIES: GENERAL — STARS: FUNDAMENTAL PARAMETERS — TECHNIQUES: HIGH ANGULAR RESOLUTION — TECHNIQUES: INTERFEROMETRIC**

1. INTRODUCTION

As the name implies, one important function of the Fine Guidance Sensors on the *Hubble* Space Telescope is to help retain precision pointing on a target while one of the other instruments on board is collecting data. The telescope is equipped with three FGS systems that collect light off of the main field of view of the science instrument cluster. The FGSs can direct light within an annulus of inner radius approximately 10 arc minutes and outer radius of approximately 14 arc minutes from the optical axis to photomultiplier detectors for collection.

One of the three FGSs, known as FGS1r, is also available for science observations and has substantial capabilities in the area of high-resolution astrometry. There are two modes of science data collection: POS, or position mode, and TRANS, or transfer mode. In the former case, positions of multiple objects that appear within the instrument field of view can be determined to high precision. In the latter case, data collection consists of determining the transfer function obtained on a single target to high precision, and then object features are deduced from the detailed shape of that function. This paper will focus only on TRANS mode observations.

TRANS mode observations are typically taken on

binary stars or stars suspected of binarity. This is because two orthogonal transfer functions are obtained by FGS, with each transfer function representing a 1-dimensional scan across the target. The double point source is simple enough to permit a unique two-dimensional solution to the image morphology. FGS has a unique combination of capabilities for binary star astronomy: separations as small as 10 to 15 milliarcseconds (mas) can be measured (depending on system magnitude), systems with magnitude as faint as 16 can be observed successfully, and magnitude differences up to 5 between the primary and secondary star can be detected. Although ground-based high-resolution imaging techniques such as speckle imaging, adaptive optics, and long baseline optical interferometry share some of these capabilities, FGS remains unparalleled in achieving this impressive combination of resolution, dynamic range, and detection limit simultaneously.

These capabilities have been used to great effect by a number of investigators in the last decade. Henry et al. (1999) have used a combination of FGS data and ground-based data to revise and substantially improve our knowledge of the lower portion of the mass-luminosity relation for nearby stars. Franz and his collaborators have studied the duplicity fraction in the Hyades (Franz et al. 1992), and pro-

¹University of Massachusetts, Dartmouth.

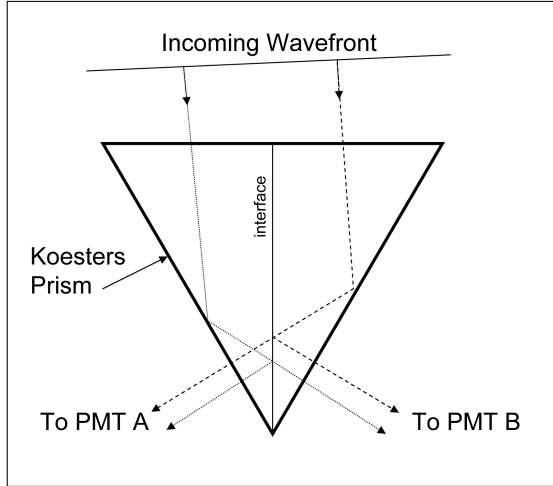


Fig. 1. The wavefront division accomplished by the Koesters Prism in the Fine Guidance Sensor system.

duced an extremely high-precision orbit of Wolf 1062 (Franz et al. 1998). In the latter work, the authors derived a mass estimate for the primary that had approximately 6% uncertainty. The primary contribution to this uncertainty came from the parallax value (where the Hipparcos parallax was used); if the parallax is measured with the means of upcoming space astrometry missions such as SIM or Gaia, a 1% mass could easily be achieved. Other representative highlights of TRANS mode FGS data analysis include orbits of Wolf 424 (Torres et al. 1999), observations of pre-main sequence stars (Bernacca et al. 1993), an analysis of serendipitous binary discoveries from guide stars (Schneider, Hershey & Wenz 1998), a negative result on a metal-poor star suspected of binarity (Osborn & Hershey 1999), and recent results on M and L dwarfs (Golimowski et al. 2004) and OB systems (Nelán et al. 2004a).

2. BASIC INSTRUMENT DESIGN

Each of the three FGSs on board *HST* is a two-axis Koesters interferometer system. The basic design of a Koesters interferometer is shown in Figure 1. Each axis contains a Koesters prism, which consists of two 30° - 60° - 90° triangular prisms cemented together along the long leg of the triangle to form an isosceles prism where the interface bisects one face of the prism. The incoming wavefront is directed toward the face containing the interface, splitting the wavefront into two pieces. The light is then totally and internally reflected off the back faces of the prism, and directed toward the interface. At contact with the interface, the light from

a given half of the prism is partially reflected and partially transmitted. Because of the symmetry of the prism, the reflected beam from one half of the prism is then combined with the transmitted portion of the beam from the other half of the prism, and vice versa. The result is that these beams travel together through focusing optics to a photomultiplier tube (PMT), where they interfere. Each prism has two exit arms, and therefore two PMTs, referred to as “A” and “B.”

If the incoming wavefront is parallel to the entrance face of the Koesters prism, then the same phase difference between the exit beams in both arms of the interferometer are reached, and that condition is intermediate between total constructive interference and total destructive interference. This arises due to the induced phase shift in the portion of the beam reflected from the central interface compared to the portion of the beam transmitted through the interface. For such a wavefront, the signal obtained from the PMTs associated with each exit arm are in theory equal. However, if the incoming wavefront is not parallel to the entrance face of the prism, then as the beam in one exit arm of the interface comes closer to the condition of destructive interference, the other arm will come closer to constructive interference, thus generating a difference in signal between the photomultipliers. Much more information concerning the optical characteristics and performance are available in Nelán et al. (2004b) and Nelán & Makidon (2004).

The FGSs are equipped with only wide filters, and indeed the science FGS (FGS1r) has only one filter option narrower than 100 nm. Therefore, the FGSs are effectively “white light” interferometers, and interference fringes wash out quickly as the incoming wavefront angle deviates from zero relative to the input face of the Koesters prism. Also, color measurements of any precision are not possible using standard photometric techniques with the filters available.

3. STANDARD TRANS MODE DATA ANALYSIS

3.1. Data Format

The raw data of FGS observations is a sequence of photons detected as a function of time on each axis of the instrument, hereafter x and y . The lower the number of counts, the closer the wavefront is to a tilt that gives rise to destructive interference, and the higher the number of counts, the closer the wavefront is to a tilt that gives rise to constructive interference. The object is translated across a fiducial position within the field of view to generate a

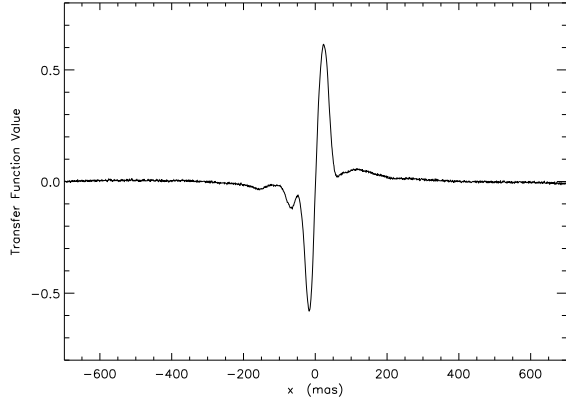


Fig. 2. Cross-correlated, co-added scans of the single star HIP 3430.

range of effective wavefront tilts so that the separation between each sample point corresponds to nominally 1 mas in position. These data arrive to the user as a FITS file that stores the samples in a two-dimensional array that is $7 \times N$ samples in size, where N is the number of time samples in the observation. The 7 “rows” then give the PMT A and B counts in the x direction (rows 1 and 2), the PMT A and B counts in the y direction (rows 3 and 4), and three rows of calibration information.

3.2. Co-Addition of Scans and Template Fitting

From the raw scans, one typically forms the transfer function, T , also known as the “S-curve,” by computing the following:

$$T = \frac{A - B}{A + B}, \quad (1)$$

where A represents the number of counts received by PMT A and B represents the number of counts in PMT B.

The standard FGS file contains dozens of back-and-forth scans across the target. The data stream is divided into individual scans, the sample points of every other scan are reversed to the standard orientation, and then these scans must be cross-correlated and co-added. An example of a co-added final product is shown in Figure 2.

After co-addition of scans, the standard analysis proceeds with a least-squares fit to a template binary star created from two single star transfer functions that are formed from a library of calibration objects. The existing library contains only a limited number of single star scans and covers only two filters, F583W and ND5.0. For the F583W filter, there are six single stars that span a color range of $B - V$

= 0.0 to 1.9, and for ND5.0, there are five objects that span the range -0.3 to 1.3.

This illustrates a significant problem in retrieving the best possible astrophysics with the FGS system, namely, the variability of the transfer function with color. It is also known that the transfer function varies in time, meaning that systematic errors are almost always the limiting factor in terms of the photometric, and to a lesser extent the astrometric information obtained, especially for objects observed near the limit of the FGS capabilities.

4. A NEW FOURIER-BASED APPROACH

Hershey (1992) developed a Fourier-based reduction method for FGS data. The basis of this approach is that the transfer function follows the convolution relationship. For each point source scanned, a copy of the transfer function is obtained centered on the location of the source. The transfer function therefore represents a point spread function, albeit an unconventional one, and deconvolution is straight-forward.

A variation on this method has been recently developed, specifically to address the color calibration issue mentioned above. The goal is to obtain color information of the components of binary stars observed with FGS without recourse to template fitting. This is possible in principle because the width of the S-curve is color dependent; that is, the separation between interference maxima and minima is determined by color. If the stars are well-separated, this width can in principle be measured with the standard analysis technique, but for the general case of blended S-curves, the signature is more clearly seen in the spatial frequency power spectrum of the S-curve. After deconvolution in the Fourier plane, the signature of binarity is a fringe pattern, but if the primary and secondary have different colors, the fringes tend to wash out at higher spatial frequencies. Figure 3 illustrates this point, where the power spectrum of simulated FGS data of a binary with a substantial color difference between the components is shown. The fringes begin to die away before signal is lost at higher spatial frequencies. This fringe washout is reasonably well approximated by an envelope that has the form related to a Butterworth function in the frequency domain, namely

$$B(u) = \frac{1}{1 + (u \cdot c)^8}, \quad (2)$$

where c is a color index factor, which increases with color difference between the components. The envelope function is then given by

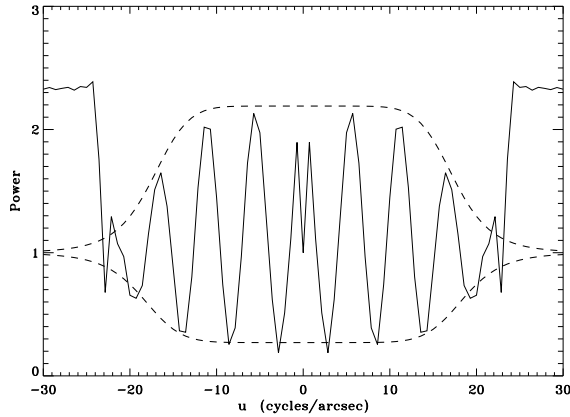


Fig. 3. Simulation results for an A0V primary and M0V secondary. The spatial frequency spectrum is shown after deconvolution by a point source. Because of the color difference, the fringe pattern indicating binarity washes out at higher spatial frequencies in a manner well-approximated by the Butterworth envelope shown by the dashed line.

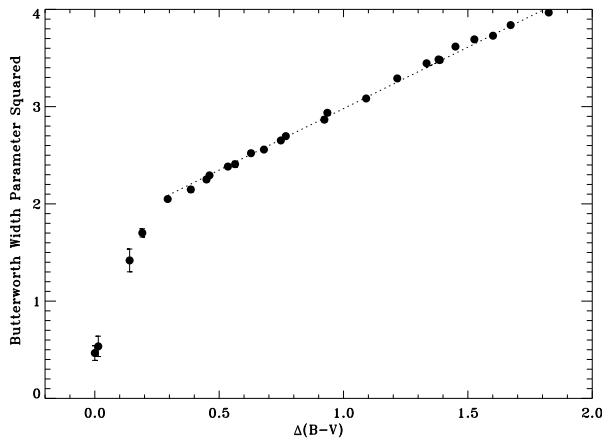


Fig. 4. Linear fit to the Butterworth width parameter squared, in the $B - V$ color difference range of 0.3 to 1.8.

$$E(u) = 1 \pm B(u) \frac{I_2}{I_1}, \quad (3)$$

where I_1 and I_2 are the intensities of the primary and secondary, respectively.

The above function can be incorporated into a scheme which fits the fringes for separation, intensity ratio, and color difference. When combined with the

second FGS axis data, position angle information can also be obtained. Although the method is very preliminary, it appears to work well at determining color differences of components of simulated FGS data. In simultaneous fitting, not only the standard binary parameters are obtained with good precision, but the color difference appears to be linearly related to the square of the color index parameter, c , mentioned above. This result is shown in Figure 4 for an A0V primary and secondaries of different colors, ranging from A0V to M6V.

I thank Otto Franz and Lawrence Wasserman (Lowell Observatory), and James Heasley (University of Hawaii) for their collaboration on the FGS data presented here. Support for Proposal numbers GO-9034 and GO-10197 was provided by NASA through a grant from the Space Telescope Science Institute, which is operated by the Association of Universities for Research in Astronomy, Incorporated, under NASA contract NAS5-26555.

REFERENCES

- Bernacca, P. L., Lattanzi, M. G., Bucciarelli, B., et al. 1993, *A&A*, 278, L47
- Franz, O. G., Henry, T. J., Wasserman, L. H., et al. 1998, *AJ*, 116, 1432
- Franz, O. G., Wasserman, L. H., Nelan, E., Lattanzi, M. G., Bucciarelli, B., & Taff, L. G. 1992, *AJ*, 103, 190
- Golimowski, D. A., Henry, T. J., Krist, J. E., et al. 2004, *AJ*, 128, 1733
- Henry, T. J., Franz, O. G., Wasserman, L. H., Benedict, G. F., Shelus, P. J., Ianna, P. A., Kirkpatrick, J. D., & McCarthy, D. W., Jr. 1999, *ApJ*, 512, 864
- Hershey, J. L. 1992, *PASP*, 104, 592
- Nelan, E. P., Walborn, N. R., Wallace, D. J., Moffat, A. F. J., Makidon, R. B., Gies, D. R., & Panagia, N. 2004a, *AJ*, 128, 323
- Nelan, E., et al. 2004b, *Fine Guidance Sensor Instrument Handbook*, Version 13.0, (Baltimore: STScI)
- Nelan, E. & Makidon, R. 2004, *HST FGS Data Handbook*, Version 4.0, ed. B. Mobasher (Baltimore: STScI)
- Osborn, W. & Hershey, J. L. 1999, *PASP*, 111, 759
- Schneider, G., Hershey, J. L., & Wenz, M. T. 1998, *PASP*, 110, 751
- Torres, G., Henry, T. J., Franz, O. G., & Wasserman, L. H. 1999, *AJ*, 117, 562